07

Nanoparticles [Ru(dipy)$_3$]$^{2+}$ @ SiO$_2$ as thermosensors and probes for luminescence tomography of biological samples

© A.V. Leontyev,[1] L.A. Nurtdinova,[1] E.O. Mitushkin,[1] A.G. Shmelev,[1] D.K. Zharkov,[1] V.V. Andrianov,[1,2] L.N. Muranova,[2] Kh.L. Gainutdinov,[1,2] R.R. Zairov,[3,4] A.R. Khasieva,[4] A.R. Mustafina,[4] V.G. Nikiforov[1]

[1] Zavoisky Physical-Technical Institute, FRC Kazan Scientific Center of RAS,
420029 Kazan, Russia
[2] Institute of Fundamental Medicine and Biology, Kazan Federal University,
420008 Kazan, Russia
[3] Alexander Butlerov Institute of Chemistry, KFU,
420008 Kazan, Russia
[4] A.E Arbuzov Institute of Organic and Physical Chemistry of Kazan Scientific Center of Russian Academy of Sciences
420088 Kazan, Russia
e-mail: vgnik@mail.ru

New luminescent nanomaterials attract tremendous interest, and in this work, silicon dioxide SiO$_2$ nanoparticles of 55 nm size containing tris(2, 2′-bipyridyl) ruthenium (II) complexes [Ru(dipy)$_3$]$^{2+}$ are tested as nanoprobes for biomedical applications. We have shown that calibration of the spectral parameters of the luminescent response based on the ratiometric method allows the use of nanoparticles in biological media as thermosensors with an accuracy of $\pm 2°$C in the biologically significant temperature range of $20-50°$C. In addition, a fluorescent tomography method has been proposed and implemented. As a result, a three-dimensional model of the surface of the grape snails nervous system was obtained with a resolution of $10\,\mu$m. This allowed us to perform a demonstration experiment - remote measurement of the local temperature of a selected area on the surface of a neuron.

Keywords: nanoluminophores, luminescent nanothermometers, nanosized bioprobes, temperature sensitivity, ratiometric method, bio-imaging, luminescent tomography.

Introduction

The creation of nanoscale sensors and probes is one of the promising and rapidly developing areas of nanotechnology. Special attention should be paid to materials in which the parameters of the luminescent response (intensity, shape of the emission spectrum, peak position, luminescence decay time, etc.) depend on the state of the local environment [1–6]. This feature allows creating luminescent sensors for remote monitoring of environmental characteristics with minimal impact on the environment, which is especially important when working with biological objects [7–10].

Temperature is one of the most important physiological parameters. To date, fluorescent proteins [11,12], quantum dots [13,14], nanodiamonds [15], gold nanoclusters [16], molecular systems [17,18] lanthanide nanoparticles [19], polymer and upconversion nanoparticles [20–22] are offered as temperature sensors with high spatial resolution Unfortunately, it is impossible to give preference to any one type of sensor suitable for a wide range of biological tasks among the rather large variety of luminescent nanomaterials, and therefore the search and development of new systems continues constantly.

Visualization is another important biomedical task, when probes embedded in a biopreparation make it possible to detect their position using luminescent spectroscopy methods, which are highly sensitive (with the possibility of registering an optical signal from a single nanoobject in photon counting mode). This technology underlies such urgent tasks as visualization of individual organs, drug transport, selective exposure to individual areas of biological tissue, test systems, etc. [23–25].

We test in this paper the suitability of 55 nm silicon dioxide nanoparticles (NP) encapsulated with tris(2, 2′-bipyridyl) ruthenium complexes (II) [Ru(dipy)$_3$]$^{2+}$ for use as fluorescent bioprobes. These NPs were proposed in Ref. [26], where their magnetic-fluorescent properties were used in experiments on controlling the activity of motor neurons obtained from the spinal cord of newborn (P1−P3) rats Wistar. The magnetic function of the NPs was provided by additional encapsulation of the NPs of superparamagnetic iron oxide. The spectral properties of [Ru(dipy)$_3$]$^{2+}$ complexes inside the silicon dioxide shell in a biologically significant temperature range of $20-50°$C were studied for expanding the functionality of NPs (without magnetic nanoparticles) for their use in a wider range of biological tasks. These studies made it possible to calibrate the spectral intensity of the NPs luminescent response
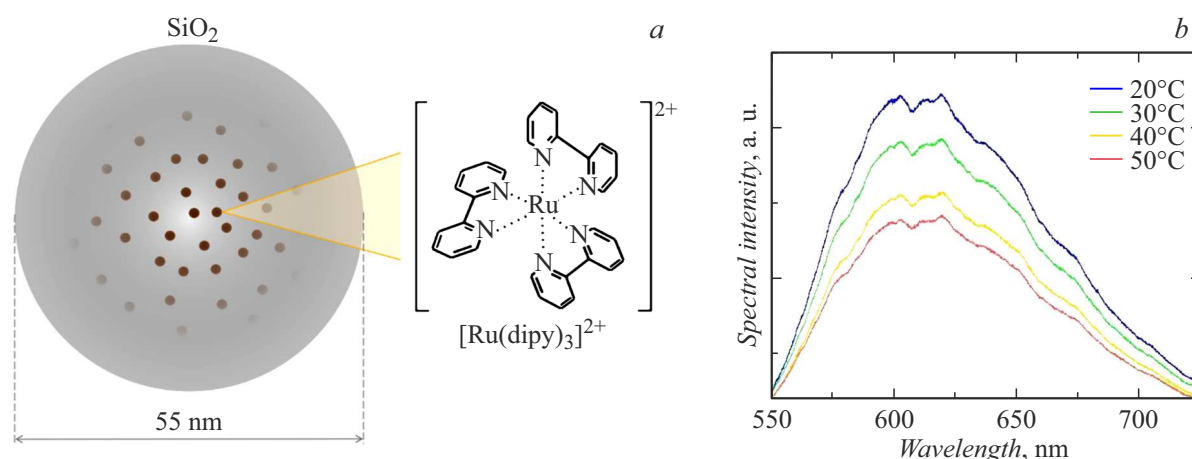
Figure 1. Schematic representation of ruthenium complexes $[Ru(dipy)_3]^{2+}$ placed in a silicon shell SiO_2 (*a*). Temperature dependence of luminescence spectra under laser excitation at a wavelength of 405 nm (*b*).

in saline solution for implementing remote temperature measurement.

Terrestrial pulmonate mollusks such as grape snails *Helix lucorum* of the Crimean population were selected for testing the calibrated NPs as thermosensors. These animals, along with other species of mollusks, are currently one of the most sought-after objects of biological research on the work of the nervous system and behavioral reactions [27,28]. In particular, grape snails are widely used in experiments analyzing learning and memory mechanisms because of their relatively simple nervous system, which nevertheless provides a rich variety of behavioral responses. Their wide range is determined by complex interactions of unconditioned reflexes modulated by the processes of habituation, sensitization and associative learning. At the same time, a rather narrow ensemble of neurons for a particular behavioral reaction reliably provides the functionality of the nervous system of the grape snail. An important factor is that the sizes of neuron bodies up to $200-300\,\mu m$ in diameter make it possible to accurately identify the location of cells of individuals of this species. This important circumstance opens up great opportunities for the implementation of various experiments using bioimaging based on fluorescent nanoprobes. In addition, an interesting feature is the superficial nature of the location of neurons in the ganglia.

We propose in this paper to use NPs as luminescent probes on living tissues of the isolated nervous system of the grape snail for implementing topographic mapping of their surface. NPs act as local luminescence sources in this technique, the position of which in a three-dimensional coordinate system is determined by optical confocal microscopy, which is capable of detecting radiation from single NPs in the photon counting mode with a lateral resolution of $1\,\mu m$. In particular, such a technique, unlike traditional magnetic resonance imaging methods with a resolution of the order of 1 mm allows for detailed examination of objects at the cellular level. A three-dimensional digital model

with a spatial resolution of $10\,\mu m$ was obtained in our luminescent tomography experiment. This made it possible not only to determine the morphology of individual sites in detail, but also to provide precision access to the objects of interest for further work with them. Since the NPs used for luminescent tomography are also temperature sensors, a demonstration experiment was performed to measure the local temperature on the surface of a separate pre-selected neuron, which was accessed using a three-dimensional model.

1. Experiment

$[Ru(dipy)_3]^{2+}$ complexes encapsulated in a shell SiO_2 with a size of $55 \pm 5\,nm$ were used as luminescent probes (Fig. 1, *a*). It is known that encapsulation of fluorescent organic or inorganic compounds in silicon nanoparticles is one of the effective ways to protect against the negative effects of surface luminescence quenchers in biological media [29,30]. The approaches used to create luminescent NPs in this paper, were described in detail in [26], where their detailed characterization was also presented.

The temperature dependence of the luminescent properties of NPs placed in a saline solution was studied using a confocal microscope. A diode laser with a wavelength of 405 nm was used as an excitation source. Laser irradiation caused intense luminescence, clearly visible to the naked eye (Fig. 1, *b*). The recording system made it possible to detect the luminescence spectrum in the wavelength range of $350-1100\,nm$. A 4x lens collecting radiation and a laser beam positioning system provided a spatial lateral resolution of the microscope $10\,\mu m$.

The data were recorded as follows in the luminescent tomography experiment. The sample, which is a living isolated nervous system of a grape snail in saline solution, was placed in the focal plane of the lens. Next, the object was scanned repeatedly using a positioning system based on a galvanometric scanner that moves a laser beam along

the surface of the sample. Axial scanning was performed by adjusting the height of the microscope slide. Thus, an array of data was collected, representing the dependence of the luminescence intensity on the coordinates of the focal spot. The area of the scanned surface was 2.7×2.7 mm. The spectrum of the recorded luminescence, shown in Fig. 1, b, and also in Ref. [26], corresponded to the characteristic wide structureless line of complexes $[Ru(dipy)_3]^{2+}$.

The isolated nervous system of the terrestrial pulmonate mollusk *Helix lucorum* (grape snail) of the Crimean population was selected as a biological preparation. The nervous system of the preparation included a subcaryngeal ganglia complex consisting of pleural, parietal, pedal and visceral ganglia. Tungsten brackets were used to fix the circumflex ring. Connective tissue sheaths on the surface of nerve cells were removed using tweezers and a miniature scalpel under a binocular microscope. The biopreparation was placed in a saline solution of the following composition: NaCl — 80 mM, KCl — 4 mM, $CaCl_2$ — 7 mM, $MgCl_2$ — 5 mM, $NaHCO_3$ — 5 mM; pH $= 7.6-7.8$.

2. Temperature calibration of nanoluminophores

It is known that in the $[Ru(dipy)_3]^{2+}$ complex, as a result of light absorption in the 405 nm region, a state with charge transfer from the metal to the ligand occurs. The relaxation process of this excited state goes through several stages. At first, the singlet excited state turns into a triplet state due to rapid intercombination processes. This is followed by transitions through the multiphonon transition and radiative relaxation. In turn, radiative transitions resulted in the appearance of a wide emission band from the orange to the near infrared range, the characteristic form of the spectrum of which is shown in Fig. 1, b [31,32].

The study of temperature dependence and verification of the possibility of remote temperature measurement were performed as follows. It is known that the aqueous medium and its temperature can have a significant effect on the luminescence parameters of NPs. Since it was not possible to vary the temperature of the NPs inside a living biological product, a saline solution was chosen as a model medium close to a living biological preparation. Thus, the NPs were placed in a saline solution, the temperature of which slowly varied in the biologically significant range of $20-50°$C. Fig. 1, b shows these very spectral intensities obtained with an optical confocal microscope.

It can be seen that the luminescence brightness, which represents the full integral intensity, has a pronounced temperature dependence. However, it is impractical to use this parameter for NP temperature calibration and subsequent temperature measurement. This is attributable to a huge number of related factors (such as the geometry of the experiment, the length of the optical path, scattering in the medium, laser parameters, parameters of the recording system, etc.), which together have a significant impact on the intensity of the recorded signal. Practically, their simultaneous control is a rather difficult task, which complicates the experiment a great deal. Neglecting these factors results in a very poor repeatability of the results due to constantly occurring systematic errors.

There is another approach using the ratiometric principle. It is based on the analysis of temperature dependences of relative intensities of various sections of the luminescence spectrum. The main advantage of the ratiometric approach is that it makes it possible to eliminate systematic errors associated with the recording of absolute values of luminescence intensity.

Thus, the ratiometric method was used as the basis for calibration of the temperature dependence of the NPs in saline solution. First, the luminescence spectra were „cleared" using the Fourier transform from the high-frequency Fourier component associated with low-amplitude random fluctuations of the signal. Next, the smoothed spectral dependencies were normalized to their maximum values. The temperature dependences of the luminescence spectra processed in this way are shown in Fig. 2, a.

In general, it is clearly seen that the spectral profile of the normalized luminescence varies quite slightly in a given temperature range. Meanwhile, there are areas where the spectral intensity significantly depends on temperature. Thus, obvious changes in the luminescence signal are present in the regions of $550-580$ and $590-610$ nm.

A comparative analysis of changes in various regions of the normalized spectral intensity with temperature was carried out to find optimal parameters. As a result, it was found that the best result in sensitivity and signal-to-noise ratio is achieved in the case of choosing R-function defined as the ratio of intensities for the spectral ranges of $555-574$ nm (I_1) and $581-582$ nm (I_2):

$$R = I_1/I_2. \qquad (1)$$

This R-function is well approximated by a linear dependence of the following form in the temperature range of $20-50°$C

$$R(T) = 0.012 \cdot T + 5.638. \qquad (2)$$

It is important to note that the expression (2) is also a calibration function for remote temperature measurement (Fig. 2, b). It was found under the conditions of our experiment, by calculating the mean square deviation based on the calibration function (2) with multiple measurements that the accuracy of temperature determination is $\pm 2°$C. It should be clarified that this value is mainly determined by the parameters of the recording system of an optical confocal microscope. It is known that the accumulation of a signal (for example, under the same conditions without increasing the recording time, but by narrowing the spectral ranges to significant regions $555-574$ nm and $581-582$ nm) can significantly increase the accuracy of temperature measurement by the proposed method.
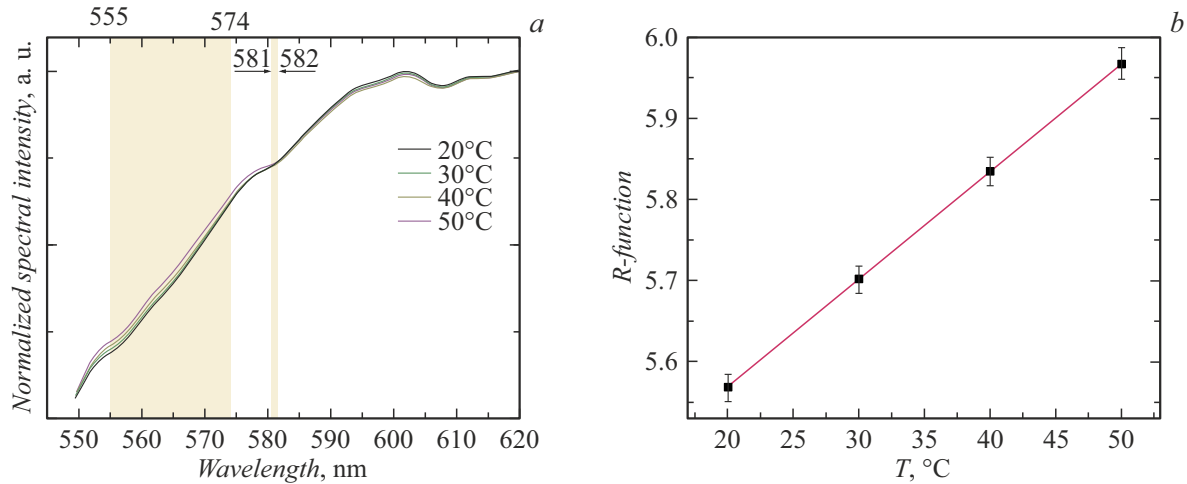
Figure 2. *a* — smoothed and normalized spectral luminescence intensities depending on temperature. The areas 555−574 and 581−582 nm are highlighted in color for calculating *R*-functions (*1*); *b* — *R*-function that can be used as a calibration for remote temperature measurement (red line). Black squares — the result of an experimental measurement.

It should be noted that, despite the relatively high absolute sensitivity of S_A in the selected temperature range

$$S_A = \frac{dR(T)}{dT} = 12 \cdot 10^{-3} \, (°C)^{-1}, \qquad (3)$$

a rather large measurement error indicates additional factors affecting the recorded luminescence. The photodegradation of NPs under the impact of intense radiation perhaps may be one of these factors. The photostability of the NPs and the effect of prolonged laser exposure have not been studied in this paper. It should be noted that the importance of such information for the practical use of NPs in the role of thermosensors, given that the intensity of laser excitation in an optical confocal microscope reaches values of the order $10^3 \, \text{W/mm}^2$ [33]. The study of the parameters and mechanisms of the proposed photodegradation is the subject of further study.

The relative sensitivity is of great importance from the point of view of practical application:

$$S_R(T) = \frac{S_A}{R(T)} = \frac{1}{T + 469.8}. \qquad (4)$$

Its maximum value in the temperature range of 20−50°C is $0.002 \, (°C)^{-1}$, which also indicates a significant dependence of the accuracy of temperature measurement on the experimental error of measuring the luminescence signal.

3. Determination of the morphology of the surface of the nervous system of the grape snail

The surface of the isolated nervous system of the grape snail was coated with luminescent NPs for implementing the luminescent tomography. 0.1 ml of an aqueous colloidal solution with a concentration of NP equal to 0.5g/l was added to the biopreparation for this purpose. Effective adsorption of SiO₂-nanoparticles on biological tissues [34] led to rapid deposition of most NPs [Ru(dipy)₃]²⁺ @ SiO₂ on the surface of the nervous system.

The configuration of the confocal microscope used ensured the recording of an optical signal from an object with an axial resolution of $10 \, \mu m$. A lateral change of the surface coordinate was achieved with a resolution of $10 \, \mu m$ using a galvanometric scanner. As a result, this technique made it possible to measure the intensity of the optical signal depending on the position on a given scanning plane (optical slice).

17 optical sections S_{XYZ} with a scanning field with the size of $2.7 \times 2.7 \, \text{mm}$ were taken for performing the tomography of the surface of the nervous system based on the recording of the luminescent response with the excitation by 405 nm laser, where S_{XYZ} — the intensity of the luminescent signal, X and Y — surface coordinates, Z — the position of the focal plane of the optical confocal microscope. The position of the Z coordinate differed in the taken 17 optical sections of the same part of the sample which provided information about the depth of the luminescent layer. Further, the array of experimental data was processed as follows. The height of the surface with the specified X- and Y-coordinates H_{XY} was determined based on the analysis of the signals of all scans:

$$H_{XY} = \frac{\sum\limits_{Z=1}^{17} Z dZ S_{XYZ}}{\sum\limits_{Z=1}^{17} S_{XYZ}}, \qquad (5)$$

where dZ — the distance between the focal planes of neighboring scans, which in experimental conditions was equal to $22 \, \mu m$. The results of the described procedure are shown in Figure 3, where an image of the same area taken with an optical microscope is also shown for
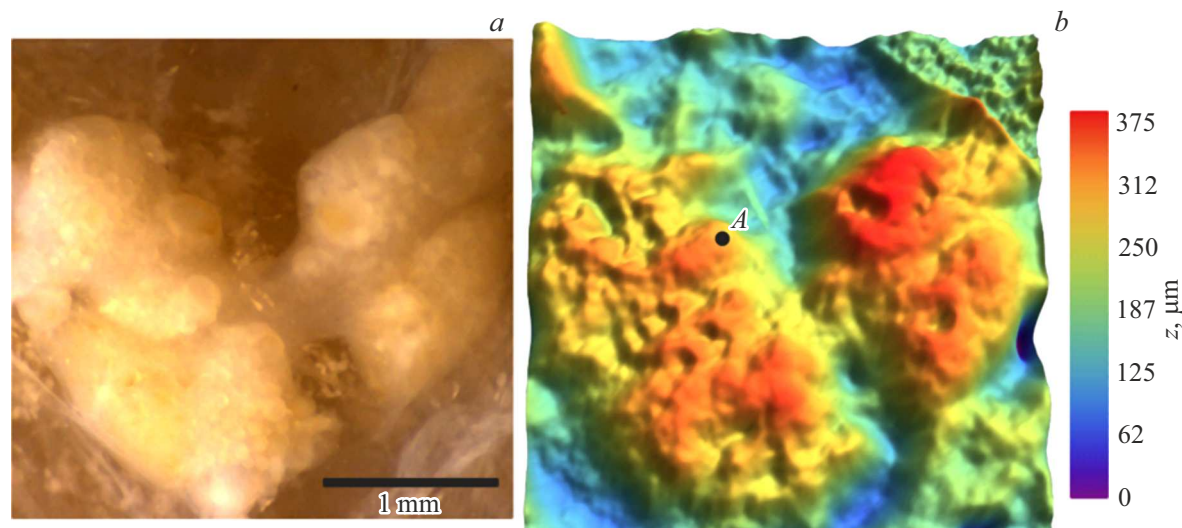
Figure 3. The surface of the subcaryngeal ganglia complex (nervous system of the grape snail). *a* — optical microscope image; *b* — three-dimensional surface of a biological sample based on layered scanning of the luminescent signal of nanoparticles $[Ru(dipy)_3]^{2+}$ @ SiO_2. The point *A* indicates the surface of the neuron where the local temperature was measured.
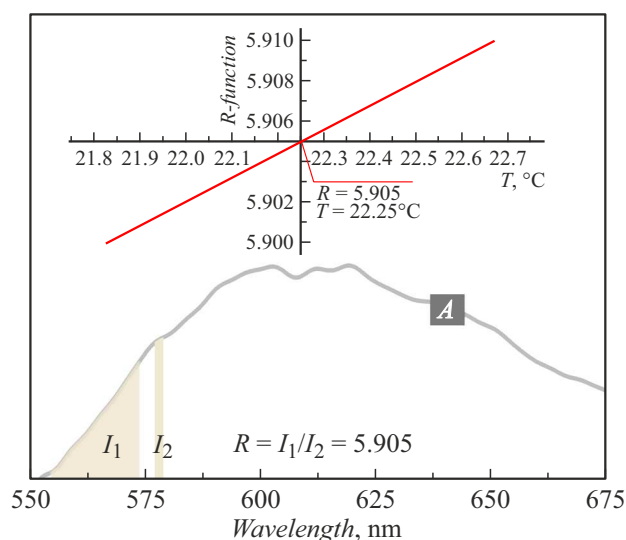
Figure 4. The NP luminescence spectrum on the surface of the nervous system of the grape snail in the region *A* in Fig. 3, on the basis of which the ratio $R = I_1/I_2 = 5.905$ is calculated. The insert shows the calibration *R*-function and evaluation of the local temperature of $T = 22 \pm 2°C$.

comparison. It can be seen that the resulting digital three-dimensional surface by processing a luminescent signal on a confocal microscope unambiguously corresponds to an optical image. Moreover, it allows obtaining much more detailed information about the morphology of the surface than a two-dimensional image of an optical microscope.

The access to any point of the scanned surface with the possibility of exposure to laser radiation or recording of an optical signal is the next promising opportunity. It is important to note that confocal microscopy methods can provide spatial resolution of up to $1\,\mu$m.

In our case, the NP used in luminescent tomography are also thermosensors, which made it possible to monitor the local temperature. Fig. 4 shows the results of a demonstration experiment on measuring temperature on the surface of a neuron — region *A* in Fig. 3, *b*. The analysis of the luminescence spectrum based on the calibration *R*-function (2) gives the value of the local temperature $22 \pm 2°C$. These data are quite consistent with the temperature of the saline solution of $23 \pm 0.5°C$, which was controlled by the classical method using a thermistor.

Conclusion

The paper presents the results of the application of the NPs $[Ru(dipy)_3]^{2+}$ @ SiO_2 with a size of $55\,$nm in the role of thermosensors and fluorescent probes suitable for use in living biological environments. A ratiometric method for remote temperature measurement is implemented based on confocal microscopy methods by calibrating the spectral features of the luminescent response. The measurement accuracy in the biologically significant temperature range of $20-50°C$ was $\pm 2°C$ under the conditions of the experiment.

A method of luminescent tomography is proposed and the surface of the living nervous system of the grape snail is mapped by applying NPs to it and scanning a luminescent signal. The resulting digital three-dimensional model with a spatial resolution of $10\,\mu$m not only reflects complete information about the morphological features of the surface, but also provides access to any point of the surface for further experiments. In particular, this made it possible to conduct a demonstration experiment on the

remote measurement of temperature on the surface of a selected neuron with an accuracy of $\pm 2°C$. In conclusion, we would like to note that the presented results, together with the paper [26], indicate the multifunctional nature and versatility of the approach to creating fluorescent NPs based on a silicon shell SiO_2 and encapsulated complexes $[Ru(dipy)_3]^{2+}$.

Acknowledgments

Funding

Conflict of interest

The authors declare that they have no conflict of interest.

References

[1] C.D.S. Brites, A. Millan, L.D. Carlos. *Lanthanides in Luminescent Thermometry* (Elsevier, 2016)

[2] C.D.S. Brites, S. Balabhadra, L.D. Carlos. Adv. Opt. Mater., **7** (5), 1801239 (2019). DOI: 10.1002/adom.201801239

[3] D. Wencel, T. Abel, C. McDonagh. Analyt. Chem., **86**, 15 (2014). DOI: 10.1021/ac4035168

[4] S. Radun, H.R. Tschiche, D. Moldenhauer, U. Resch-Genger. Sens. Actuators. B., **251**, 490 (2017). DOI: 10.1016/j.snb.2017.05.080

[5] Y. Choi, L. Kotthoff, L. Olejko, U. Resch-Gender, I. Bald. ACS Appl. Mater. Interfaces., **10** (27), 23295 (2018). DOI: 10.1021/acsami.8b03585

[6] A.G. Shmelev, D.K. Zharkov,A.V. Leontyev,V.G. Nikiforov,D.N. Petrov, M.F. Krylov, J.E. Clavijo, V.S. Lobkov.Bull. Russ. Acad. Sci. Phys., **86** (12), 1463 (2022). DOI: 10.3103/S1062873822120243

[7] A.G. Shmelev,V.G. Nikiforov, D.K. Zharkov,V.V. Andrianov,L.N. Muranova,A.V. Leontyev, Kh.L. Gainutdinov, V.S. Lobkov,M.H. Alkahtani, P.R. Hemmer. Bull. Russ. Acad. Sci. Phys., **84** (12) 1439 (2020). DOI: 10.3103/S1062873820120357

[8] D.K. Zharkov,E.O. Mityushkin, A.V. Leontiev,L.A. Nurtdinova,A.G. Shmelev,N.M. Lyadov, A.V. Pashkevich,A.P. Saiko, O.K. Khasanov,V.G. Nikiforov. Bull. Russ. Acad. Sci. Phys., **87**, 1817 (2023). DOI: 10.1134/S1062873823704191

[9] P. Lu, J. Ai. Talanta Open., **8**, 100248 (2023). DOI: 10.1016/j.talo.2023.100248

[10] J.V. Jun, D.M. Chenoweth, E.J. Petersson. Org. Biomol. Chem., **18** (30), 5747 (2020). DOI: 10.1039/d0ob01131b

[11] J.S. Donner, S.A. Thompson, M.P. Kreuzer, G. Baffou, R. Quidant. Nano Lett., **12** (4), 2107 (2012). DOI: 10.1021/nl300389y

[12] S. Kiyonaka, T. Kajimoto, R. Sakaguchi, D. Shinmi, M. Omatsu-Kanbe, H. Matsuura, H. Imamura, T. Yoshizaki, I. Hamachi, T. Morii,Y. Mori. Nature Meth., **10**, 1312 (2013). DOI: 10.1038/nmeth.2690

[13] J. Yang, H. Yang, L. Lin. ACS Nano, **5**, 5067 (2011). DOI: 10.1021/nn201142f

[14] L.M. Maestro, E.M. Rodriguez, F.S. Rodriguez, M.C. Iglesias-de la Cruz, A. Juarranz, R. Naccache, F. Vetrone, D. Jaque, J.A. Capobianco, J.G. Sole. Nano Lett., **10**, 5109 (2010). DOI: 10.1021/nl1036098

[15] G. Kucsko, P.C. Maurer, N.Y. Yao, M. Kubo, H.J. Noh, P.K. Lo, H. Park, M.D. Lukin. Nature, **500**, 54 (2013). DOI: 10.1038/nature12373

[16] L. Shang, F. Stockmar, N. Azadfar, G.U. Nienhaus. Angew. Chem. Int. Ed., **52**, 11154 (2013). DOI: 10.1002/anie.201306366

[17] S. Arai, S.-C. Lee, D. Zhai, M. Suzuki, Y.T. Chang. Sci. Reports, **4**, 6701 (2014). DOI: 10.1038/srep06701

[18] S. Arai, M. Suzuki, S.J. Park, J.S. Yoo, L. Wang, N.-Y. Kang, H.-H. Ha, Y.-T. Chang. Chem. Commun., **51**, 8044 (2015). DOI: 10.1039/C5CC01088H

[19] R.R. Zairov, A.P. Dovzhenko, A.S. Sapunova, A.D. Voloshina, K.A. Sarkanich, A.G. Daminova, I.R. Nizameev, D.V. Lapaev, S.N. Sudakova, S.N. Podyachev, K.A. Petrov, A. Vomiero, A.R. Mustafina. Sci Rep., **10** (1), 20541 (2020). DOI: 10.1038/s41598-020-77512-1

[20] T. Tsuji, S. Yoshida, A. Yoshida, S. Uchiyama. Analyt. Chem., **85**, 9815 (2013). DOI: 10.1021/ac402128f

[21] T. Hayashi, N. Fukuda, S. Uchiyama, N. Inada. PLoS ONE., **10** (2), e0117677 (2015). DOI: 10.1371/journal.pone.0117677

[22] P. Li, M. Jia, G. Liu, A. Zhang, Z. Sun, Z. Fu. ACS Appl. Bio Mater., **2** (4), 1732 (2019). DOI: 10.1021/acsabm.9b00115

[23] H.S. Lahoti, S.D. Jogdand. Cureus, **14** (9), e28923 (2022). DOI: 10.7759/cureus.28923

[24] P. Bon, L. Cognet. ACS Photonics, **9** (8), 2538 (2022). DOI: 10.1021/acsphotonics.2c00606

[25] J. Wallyn, N. Anton, S. Akram, T.F. Vandamme. Pharm Res., **36** (6), 78 (2019). DOI: 10.1007/s11095-019-2608-5

[26] S. Fedorenko, A. Stepanov, G. Sibgatullina, D. Samigullin, A. Mukhitov, K. Petrov, R. Mendes, M. Rummeli, L. Giebeler, B. Weise, T. Gemming,I. Nizameev, K. Kholin, A. Mustafina. Nanoscale, **11** (34), 16103 (2019). DOI: 10.1039/C9NR05071J

[27] P.M. Balaban. Neurosci. Biobehav. Rev., **26** (5), 597 (2002). DOI: 10.1016/S0149-7634(02)00022-2

[28] V.V. Andrianov, T.K. Bogodvid, I.B. Deryabina, A.N. Golovchenko, L.N. Muranova, R.R. Tagirova, A.K. Vinarskaya, K.L. Gainutdinov. Front. Behav. Neurosci., **9**, 1 (2015). DOI: 10.3389/fnbeh.2015.00279

[29] A.R. Mustafina, S.V. Fedorenko, O.D. Konovalova, A.Yu. Menshikova, N.N. Shevchenko, S.E. Soloveva, A.I. Konovalov, I.S. Antipin. Langmuir, **25** (5), 3146 (2009). DOI: 10.1021/la8032572

[30] S.V. Fedorenko, O.D. Bochkova, A.R. Mustafina, V.A. Burilov, M.K. Kadirov, C.V. Holin, I.R. Nizameev, V.V. Skripacheva, A.Y. Menshikova, I.S. Antipin, A.I. Konovalov. J. Phys. Chem. C, **114** (14), 6350 (2010). DOI: 10.1021/jp912225u

[31] V. Balzani, G. Bergamini, S. Campagna, F. Puntoriero.*Photochemistry and Photophysics of Coordination Compounds* (Springer, Berlin, Heidelberg, 2007)

[32] N.D. McClenaghan, Y. Leydet, B. Maubert, M.T. Indelli, S. Campagna. Coord. Chem. Rev., **249**, 1336 (2005). DOI: 10.1016/j.ccr.2004.12.017

[33] D.K. Zharkov, A.V. Leontyev, A.G. Shmelev, L.A. Nurtdinova, A.P. Chuklanov, N.I. Nurgazizov, V.G. Nikiforov. Micromachines, **14**, 1075 (2023). DOI: 10.3390/mi14051075

[34] A. Rimola, D. Costa, M. Sodupe, J.-F. Lambert, P. Ugliengo. Chem. Rev., **113** (6), 4216 (2013). DOI: 10.1021/cr3003054

Translated by EgoTranslating